



Shahrood University of  
Technology



Iranian Society of  
Mining Engineering  
(IRSM)

## An Experimental-Intelligent Method to Predict Noise Value of Drilling in Dimension Stone Industry

Reza Mikaeil<sup>1</sup>, Mostafa Piri<sup>2</sup>, Sina Shaffiee Haghshenas<sup>3\*</sup>, Nicola Careddu<sup>4</sup>, and Hamid Hashemolhosseini<sup>5</sup>

1. Department of Mining and Engineering, Faculty of Environment, Urmia University of Technology, Urmia, Iran

2. Department of Mining Engineering, Isfahan University of Technology (IUT): Isfahan, Iran

3. Department of Civil Engineering, University of Calabria, 87036 Rende, Italy

4. Department of Civil, Environmental Engineering and Architecture (DICAAR): University of Cagliari; Institute of Environmental Geology and Geoengineering, IGAG, CNR, Via Marengo 2, 09123 Cagliari, Italy

5. Department of Civil Engineering, Isfahan University of Technology (IUT): Isfahan, Iran

### Article Info

Received 10 July 2022

Received in Revised form 2  
September 2022

Accepted 12 September 2022

Published online 12 September  
2022

DOI: [10.22044/jme.2022.12092.2206](https://doi.org/10.22044/jme.2022.12092.2206)

### Keywords

Drilling noise

Dimension stone

Intelligent systems

ANFIS-SCM

ANFIS-FCM

### Abstract

The noise of drilling in the dimension stone business is unbearable for both the workplace and the people who work there. In order to reduce the negative effects drilling has on the health of the environment, the drilling noise has to be measured, assessed, and controlled. The main purpose of this work is to investigate an experimental-intelligent method to predict the noise value of drilling in the dimension stone industry. For this purpose, 135 laboratory tests are designed on five types of rocks (four types of hard rock and one type of soft rock): and their results are measured in the first step. In the second step, due to the unpredicted and uncertain issues in this case, artificial intelligence (AI) approaches are applied, and the modeling is conducted using three intelligent systems (IS): namely an adaptive neuro-fuzzy inference system-SCM (ANFIS-SCM): an adaptive neuro-fuzzy inference system-FCM (ANFIS-FCM): and the radial basis function network (RBF) neural network. 75% of the samples are considered for training, and the rest for testing. Several models are constructed, and the results indicate that although there is no significant difference between the models according to the performance indices, the proposed construction of ANFIS-SCM can be considered as an efficient tool in the evaluation of drilling noise. Finally, several scenarios are designed with different input modes, and the results obtained prove that the types of rock and the drill bits are more important than the operational characteristics of the machine.

### 1. Introduction

Consumer demand for dimension stone in the global building and civil engineering industries has been increasing consistently over the last several decades [1]. This is clear from how quickly tools and methods for working with dimension stone have changed in the last few decades. Noise pollution is a major form of environmental pollution with potential effects on the health of humans and other living organisms [2-7]. Although the expansion of this industry has had many economic benefits, these developments have always faced many challenges [8]. One of these challenges is the evaluation and control of the noise value of drilling in the dimension stone industry.

Noise exposure, whether it is audible or not, can lead to hearing loss, problems with hearing, trouble sleeping, more stress hormones being released, heart problems, irritability, and other mental health issues. Over the last century, the advent and growing use of many types of machines and vehicles has transformed the human life. According to the World Health Organization (WHO): noise pollution is the third most common environmental risk factor, after air and water pollution [9]. Noise pollution has a wide range of adverse effects on not only humans but also other living organisms. Extensive studies, especially in the field of occupational exposure, indicate that

✉ Corresponding author: [Sina.shaffieehaghshenas@unica.it](mailto:Sina.shaffieehaghshenas@unica.it) (S. Shaffiee Haghshenas).

noise directly affects the human auditory system. One of the major types of noise is the noise generated by drill bit-rock surface interactions during drilling operations [10]. Drilling noises are known to have adverse effects on the workers. The characteristics of these noises can also serve as an indicator of the performance of drilling tools [11]. Noises and acoustic waves are often used to figure out what is wrong with machines, and less often, to figure out what rocks are like [12]. Obert and Duvall (1941) (1942) have used acoustic emissions (sound waves) to predict the blast characteristics of rock in mining operations [13, 14]. Later, other researchers studied the changes in the acoustic wave amplitude in a frequency band with the increase in stress [15-18]. In the studies conducted by Zborovjan (2002) and Zborovjan *et al.* (2003): the hidden Markov model of acoustic signals in different types of rock has been used to identify the type of rock for drilling operations [19-20]. Gradl *et al.* (2008) have used a standard microphone to record and analyze the vibrational properties of the noise made when the bit hit the rock during drilling [10]. Vardhan *et al.* (2009) have tried to use the sound level produced during drilling in a laboratory scale rock sample to estimate the compressive strength and abrasion resistance of the rock [21]. Yilmaz and Kaynar (2010) have used Artificial Neural Networks (ANNs) of the Multi-Layer Perceptron (MLP) and Radial Basis Function (RBF) types and Adaptive Neuro-Fuzzy Inference System (ANFIS) to predict soil swelling, and compared the results with the results of traditional multiple regression [22]. In a study by Kumar *et al.* (2011): they developed a general prediction model for the relationships between the sound level generated during the drilling of sedimentary rocks and their physical-mechanical properties such as uniaxial compressive strength, tensile strength, and porosity [23]. Kumar *et al.* (2013) have used soft computing techniques such as multiple regression and artificial neural networks to predict rock properties based on a set of inputs including drill rotation speed, penetration rate, drill bit diameter, and equivalent sound level during drilling [24]. Kahraman *et al.* (2013) have used the measured sound levels to predict the abrasion resistance of rocks [25]. In a study by Masood (2015): the sound level generated during the excavation of igneous rocks with a portable drilling machine was

modeled [26]. Delibalta *et al.* (2015) have used the noise levels measured during the diamond sawing process to predict the physical and mechanical properties of the sawed rock [27]. Kivade *et al.* (2015) have developed an ANN model for predicting the properties of sedimentary rock based on the penetration rate and sound level generated during percussive drilling [28]. In another study, Kumar *et al.* (2019) have developed a new method for estimating rock properties based on the dominant frequencies of the noise produced during the diamond core drilling operation [29]. In a series of studies by Yari and Bagherpour (2018, 2019): the Fourier transform was used to model the relationship between the rock mass characteristics and the dominant frequencies of the sound waves generated during drilling [30-32]. Piri *et al.* (2021) have studied and compared the sound levels generated during drilling with three types of bit in three hard rock samples [33].

Reviewing the past studies shows that, even though a lot of research works has been done in this area, more research work is required to find out if intelligent ways can be used to cut down on the noise pollution caused by the stone industry.

## 2. Methodology

This work aimed to investigate the factors affecting the sound level generated in this industry. To reach this goal, 135 lab tests were done on three groups of hard rock (granite) samples using a drill machine with different production rates, rotation speeds, and drill bits with different levels of hardness. The noise made during each test was measured. In order to achieve the best mapping between the input and output data, the measured data was analyzed using three intelligent methods: Adaptive Neuro-Fuzzy Inference System-Subtractive Clustering Method (ANFIS-SCM); Adaptive Neuro-Fuzzy Inference System-Fuzzy c-means (ANFIS-FCM); and RBF artificial neural network. Next, the models developed by these methods were examined and compared in order to determine which one performed better in predicting the noise level. Finally, the chosen model was used to examine the factors that influenced the noise value of drilling in multiple scenarios. A diagram of the stages of this work is illustrated in Figure 1.

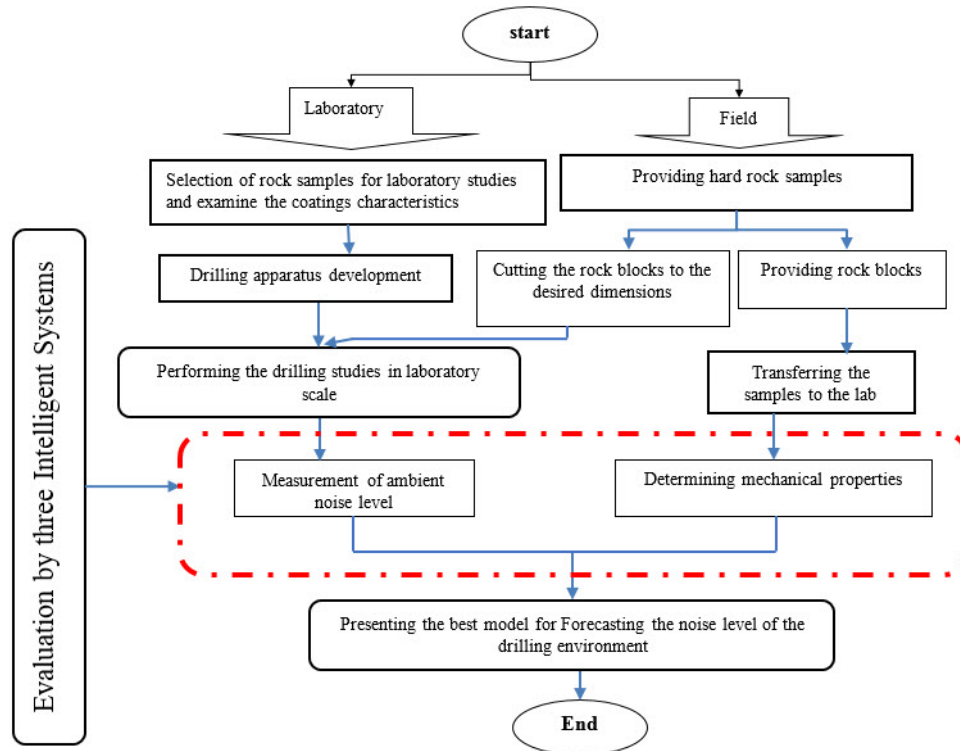


Figure 1. Research methodology flow chart.

2.1. Laboratory and field studies

This work used three types of drill bits in the tests: a bit with WC coating, a bit with TiSiAl coating, and a bit with Diamond-DLC coating. Five kinds of rocks including Khoshaintat granite, Khorramdarreh granite, white Natanz granite,

Nehbandan granite, and marble, were used in these tests. A drilling machine made to measure the drilling parameters was used to drill into these rocks. Before the tests, four primary mechanical properties of the rocks were measured. The results of these rock mechanics measurements are given in Table 1.

Table 1. Important mechanical properties of rocks.

| Commercial name | Name of quarry | Uniaxial compressive strength (MPa) | Schmiazek abrasivity factor (N/mm) | Mohs hardness (N) | Young's modulus (GPa) |
|-----------------|----------------|-------------------------------------|------------------------------------|-------------------|-----------------------|
| Granite         | Khoshtinat     | 133                                 | 10.42                              | 5.65              | 28.9                  |
| Granite         | Khoramdareh    | 141                                 | 11.1                               | 5.67              | 36.5                  |
| Granite         | Sefid natanz   | 150                                 | 13.4                               | 5.7               | 43                    |
| Granite         | Nehbandan      | 155                                 | 14.84                              | 5.95              | 39                    |
| Marble          | Salsali        | 68                                  | 0.105                              | 3.1               | 31.6                  |

All drilling tests were performed in a laboratory. The sound generated during the drilling of different rocks with different drill bits was measured by a sound level meter.

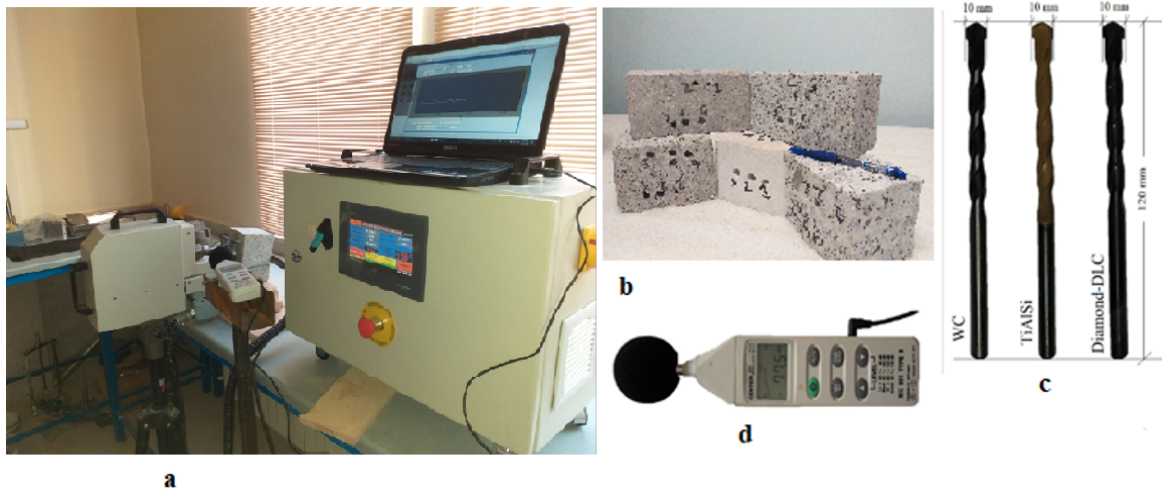
Since noise was measured at a certain time, the average amount of noise measured for each sample of rock was written down for each drilling test, taking into account the different operational parameters and the hardness of the drill bit. For example, the mean value was 92.79 for Nehbandan granite rock drilled with a drill with a Diamond-DLC coating at a penetration rate of 18 mm/min

and a rotation speed of 950 rpm. Since the base noise level of the test environment and the drilling machine was measured to be 75–80 dB, before any analysis or comparison, the average of these figures (77.5 dB) was deducted from all measured noise levels. The results of the measured noise for Nehbandan granite rock with respect to various operational parameters and drill bit hardness are presented in Table 2.

Figure 2 displays a picture of the drilling machine, the rock samples, the drill bits, and the noise level meter used in the work.

**Table 2. Results of measured noise for Nehbandan granite rock.**

| Bit         | Penetration rate (m/min) | Speed of rotation (rpm) | Noise value (db) | Environment noise value (db) | Noise value of drilling (db) |
|-------------|--------------------------|-------------------------|------------------|------------------------------|------------------------------|
| TiAlSi      | $12 \times 10^{-3}$      | 850                     | 88.45            | 77.5                         | 10.95                        |
|             |                          | 900                     | 87.88            | 77.5                         | 10.38                        |
|             |                          | 950                     | 89.41            | 77.5                         | 11.91                        |
|             | $18 \times 10^{-3}$      | 850                     | 89.67            | 77.5                         | 12.17                        |
|             |                          | 900                     | 88.86            | 77.5                         | 11.36                        |
|             |                          | 950                     | 89.74            | 77.5                         | 12.24                        |
|             | $24 \times 10^{-3}$      | 850                     | 88.08            | 77.5                         | 10.58                        |
|             |                          | 900                     | 90.55            | 77.5                         | 13.05                        |
|             |                          | 950                     | 91.03            | 77.5                         | 13.53                        |
| Diamond-DLC | $12 \times 10^{-3}$      | 850                     | 92.04            | 77.5                         | 14.54                        |
|             |                          | 900                     | 93.86            | 77.5                         | 16.36                        |
|             |                          | 950                     | 92.42            | 77.5                         | 14.92                        |
|             | $18 \times 10^{-3}$      | 850                     | 92.39            | 77.5                         | 14.89                        |
|             |                          | 900                     | 94.27            | 77.5                         | 16.77                        |
|             |                          | 950                     | 92.79            | 77.5                         | 15.29                        |
|             | $24 \times 10^{-3}$      | 850                     | 93.29            | 77.5                         | 15.79                        |
|             |                          | 900                     | 92.67            | 77.5                         | 15.17                        |
|             |                          | 950                     | 93.24            | 77.5                         | 15.74                        |
| WC          | $12 \times 10^{-3}$      | 850                     | 95.4             | 77.5                         | 17.9                         |
|             |                          | 900                     | 96.18            | 77.5                         | 18.68                        |
|             |                          | 950                     | 98.28            | 77.5                         | 20.78                        |
|             | $18 \times 10^{-3}$      | 850                     | 95.75            | 77.5                         | 18.25                        |
|             |                          | 900                     | 96.2             | 77.5                         | 18.7                         |
|             |                          | 950                     | 98.13            | 77.5                         | 20.63                        |
|             | $24 \times 10^{-3}$      | 850                     | 96.95            | 77.5                         | 19.15                        |
|             |                          | 900                     | 97.7             | 77.5                         | 20.2                         |
|             |                          | 950                     | 98.56            | 77.5                         | 21.06                        |

**Figure 2. An overview of a) drilling machine; b) rock samples c) drill bits; and d) noise measurement device.**

**2.2. Intelligent systems**

**2.2.1. Radial basis function network (RBF) neural network**

In recent decades, artificial neural networks have greatly contributed to progress in many fields of science and engineering, as well as technological advancement in a wide range of industries [34-45]. The Radial Basis Function (RBF) neural network is a strong and effective artificial neural network that can solve many complex problems. This network is a feed-forward network. Most feed-forward networks have three layers: the input layer, the hidden layer, and the output layer. It was

introduced by Moody and Darken in 1980 [46-47]. The input layer transforms the input data into a vector of real numbers, which is then processed by a hidden layer with radial basis functions as activation functions. The output of this network in the last layer (output layer) can be a linear combination of radial basis functions for input parameters and neurons [48-49]. RBF neural networks are used in several areas, including classification, time series prediction, function approximation, and system control. Figure (3) shows the general form of an RBF neural network with three layers.

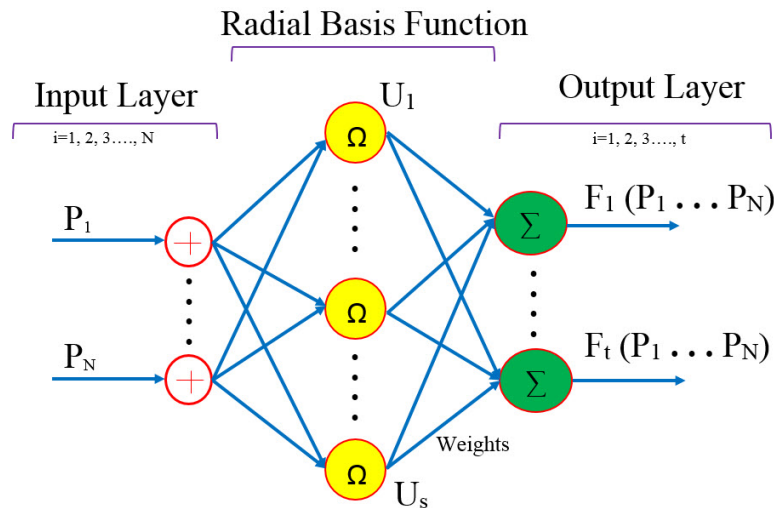


**Figure 3. Basic form of RBF neural network.**

As shown in Figure 3, the RBF network receives data in the form of input vectors  $P_1, P_2, \dots, P_N$  uses them for training/processing in the hidden layer, and ultimately produces a solution in the form of output vector  $F_1, F_2, \dots, F_t$  in the output layer [50]. The feature that distinguishes the RBF network from other neural networks is how it processes the data in the hidden layer. Although an RBF network requires more neurons than a conventional MLP, it is much faster to build and train.

**2.2.2. Adaptive network-based fuzzy inference system**

Intelligent systems play an important role in solving the engineering problems under conditions that are unpredictable and uncertain. Many researchers and engineers from different fields have used these intelligent systems to solve difficult problems and find the best solutions [51-64]. One of these intelligent systems is the

Adaptive Network-Based Fuzzy Inference System (ANFIS): which includes a combination of the capabilities of fuzzy systems and artificial neural networks [65]. When classical mathematics such as differential equations does not have the capability for modelling complex systems, ANFIS can be considered as an efficient and powerful tool for modelling in these cases [66-68]. ANFIS was first introduced in 1993 by Jang [69-70]. Using the input-output data and the learning process, it is also a powerful tool for estimating functions [71]. After the introduction of ANFIS, the various structures of it were presented, which work and model based on some kinds of data clustering including the evolving fuzzy neural networks, the dynamic evolving neural-fuzzy, the generic self-organizing fuzzy neural network (GenSoFNN); and the self-adaptive fuzzy inference network (SAFIN) [72]. The basic structure of ANFIS with five layers is shown in Figure 4.

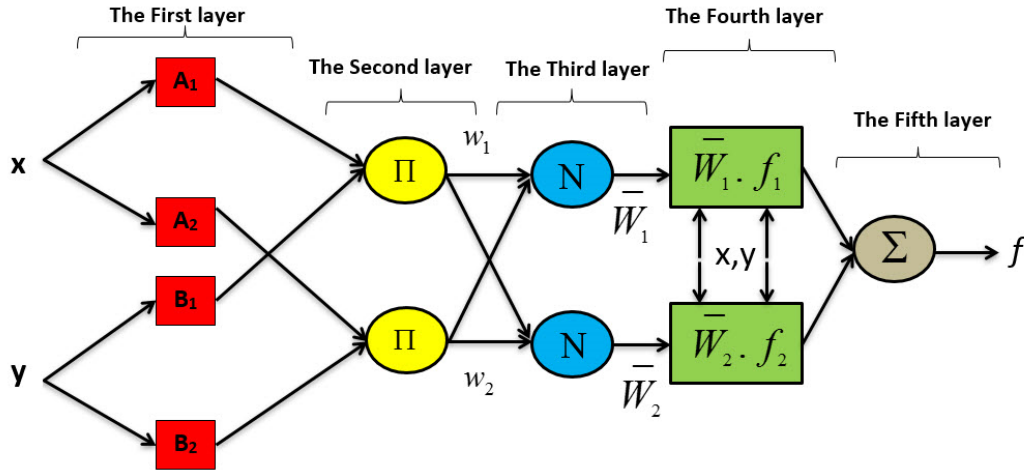


Figure 4. A basic form of ANFIS model.

The first layer contains the input nodes. According to Equation 1, each node generates the membership degree values of each input using the membership functions (MFs). In Equation 1,  $Q_{l,i}$  and  $\mu$  represent the membership degree of the fuzzy set and the membership function, respectively.  $X$  and  $Y$  are the inputs that represent  $A$  and  $B$  as the linguistic labels [71, 72].

$$Q_{l,i} = \mu A_i(x) \text{ for } i = 1,2$$

or

$$Q_{l,i} = \mu B_{i-2}(y) \text{ for } i = 3,4 \tag{1}$$

The output value in the second layer (nodes of rules) is gained by multiplying the input signals according to Equation (4) that is shown by  $\Pi$  label based on Equation 2. It is worth noting that the output of each node in this layer expresses the firing strength of each rule [71, 72].

$$Q_{2,1} = w_i = \mu A_i(x_i) \cdot \mu B_i(x_i) \text{ for } i=1,2 \tag{2}$$

In the third layer, the ratio of the firing strength of each rule for the  $i$ th node to the firing strength of the total rules is calculated based on Equation 3. Each node in this layer is introduced with  $N$  label.

$Q_{3,i} (\bar{w}_i)$  is normalized firing strengths that is the output of this layer [72, 73].

$$Q_{3,1} = \bar{w}_i = \frac{w_i}{\sum_{j=1}^2 w_j} \text{ for } i=1,2 \tag{3}$$

In the fourth layer, every node is considered an adaptive node that is matched with the node

function based on Equation 4.  $\bar{w}_i$  is the output of the third layer, and  $p_i, q_i$  and  $r_i$  represent a set of parameters of the node function, which are known as the inductive parameters of the fuzzy model section [71, 72].

$$Q_{4,1} = \bar{w}_i \cdot f_i = \bar{w}_i(p_i x + q_i y + r_i) \tag{4}$$

In the final layer, there is only one node that is marked with the  $\Sigma$  label. This node consists of the sum of the all signals of the output of the previous layer, and provides an output that corresponds to Equation 5. It is worth noting that in this layer the result is presented as a non-fuzzy output using the defuzzifier rules [71, 72].

$$Q_{5,1} = \sum \bar{w}_i \cdot f_i = \frac{\sum w_i \cdot f_i}{\sum w_i} \tag{5}$$

### 2.2.3. Fuzzy C-Means (FCM) clustering approach

The process that separates the components of a set into different groups is generally called clustering [73]. In this process, the components of each group have the most similar properties to each other. The clustering algorithms all work in a similar way but they use different ways to figure out how far apart each group's members are from the center of each cluster. The clustering algorithms are also classified into two general forms: fuzzy and classical. In classical clustering, the members belong to only one class, while in fuzzy clustering, each member can belong to different classes based on different membership degrees [74]. There are several fuzzy clustering algorithms that are considered flexible clustering techniques and have successful applications in

solving machine learning problems. One of the most efficient fuzzy clustering algorithms is the fuzzy C-means (FCM). In fact, it is an extension of the Hard C-mean (HCM) method, and was introduced by Bezdek [75].

Before starting the algorithm process, the number of classes is specified, which is indicated by "C" and its value is at least 2 and more. Then the weighting factor (m') value is assigned, which indicates the values of fuzziness in the clustering process. At the beginning process of the algorithm, the initial partition matrix (U(0)) is guessed, and then the number of iterations of the algorithm is determined that is shown with r. In each iteration, the center of each clusters {Vi(r)} is calculated, which represents the coordinates of each cluster. The partition matrix is updated as Ū(r) after the rth iteration [75]. This process is performed based on Equations 6 to 10.

$$\mu_{ik}^{(r+1)} = \left[ \sum_{j=1}^c \left( \frac{d_{ik}^{(r)}}{d_{jk}^{(r)}} \right)^{\frac{2}{(m'-1)}} \right]^{-1} \tag{6}$$

for  $I_k = \varphi$

$$\mu_{ik}^{(r+1)} = 0 \tag{7}$$

for all classes i where  $i \in \tilde{I}_k$

$$I_k = \{i | 2 \leq C \leq n; d_{ik}^{(r)} = 0\} \tag{8}$$

$$\tilde{I}_k = \{1, 2, 3, \dots, c\} - I_k \tag{9}$$

$$\sum_{i \in I_k} \mu_{ik}^{(r+1)} = 1 \tag{10}$$

where  $\mu_{ik}^{(r+1)}$  expresses the membership degree of the kth member in the ith cluster for r + 1 iteration of clustering process.  $d_{ik}$  represents the Euclidean distance between the center of the kth member and the ith cluster. In the last step of the clustering process, the accuracy of algorithm is assessed. If Equation 11 is met, the clustering process will be stopped; otherwise, the process is started from the first step, and this process is repeated till Equation 11 is met [75].

$$\|\tilde{U}^{(r+1)} - \tilde{U}^{(r)}\| = \varepsilon_L \tag{11}$$

**2.2.4. Subtractive clustering method (SCM)**

The subtractive clustering method is one of the efficient methods of clustering that was introduced by Chiu. The clustering process in this algorithm is based on the fact that all points can be a potential cluster center. Initially, for a set, the number of

clusters and the cluster centers are estimated. Then the numbers of subtractive centers were used to make automatic MFs, rule base, and the position of MF within dimensions [76].

Hence in the m-dimensional space, a set of points {X1, X2, X3, ..., Xn} is determined for which each Xi can be considered as a cluster center. For each Xi, a density measure is calculated based on Equation 12 [71, 72].

$$D_i = \sum_{j=1}^n \exp \left( - \frac{\|x_i - x_j\|^2}{\left(\frac{r_b}{2}\right)^2} \right) \tag{12}$$

where  $D_i$  represents a density measure, and  $r_a$  expresses a neighborhood radius, which is a positive constant for each data point examined. Therefore, when a data point has a high-density value in its neighborhood radius, it shows that there are a large number of neighboring data points in this domain (radius). In addition, the data points that are outside the radius of  $r_a$  have a low impact level on the density value, although they do not have a significant and direct impact on calculating the density value. Then the first center of a cluster belongs to a data point with the highest density among all data points, and  $X_{c1}$  and  $D_{c1}$  are calculated to introduce the center and density of the first cluster. Then the density of each data point is calculated based on Equation 13 [71, 72].

$$D_i = D_i - D_{c1} \sum_{j=1}^n \exp \left( - \frac{\|x_i - x_{c1}\|^2}{\left(\frac{r_b}{2}\right)^2} \right) \tag{13}$$

where  $r_b$  determines a neighborhood including measurable decreases in the density measure, and it is a positive constant. This process is done to determine the density and coordinates of the next data point, and then this process is updated to finally reach the desired number of clusters with the most optimal value in density and coordinates.

**3. Modeling**

A performance evaluation was performed in terms of three measures to ensure that the models have been developed properly and to check and compare their accuracy. These measures were the Variance Account For (VAF): Root Mean Square Error (RMSE): and Coefficient of Determination ( $R^2$ ): which were calculated by Equations 14-16.

$$VAF = \left[ 1 - \frac{var(x_i - y_i)}{var(x_i)} \right] \tag{14}$$

$$RMSE = \sqrt{\frac{1}{n} \sum_{i=1}^n (x_i - y_i)^2} \quad (15)$$

$$R^2 = \frac{[\sum_{i=1}^n (x_i - x_{mean})^2] - [\sum_{i=1}^n (x_i - y_i)^2]}{[\sum_{i=1}^n (x_i - x_{mean})^2]} \quad (16)$$

The model was developed with seven inputs, of which four were the mechanical properties of the rock, namely its uniaxial compressive strength, Mohs hardness, Schimazek's F-abrasiveness factor, and Young modulus. One was the main characteristic of the drill bit, i.e. its hardness, and two were operational characteristics of the drill machine, namely its production rate and rotation speed. The output of the model was the noise of drilling. Of the datasets collected from 135 tests, 75% (101 datasets) were used to train the model, and the rest were used to test the model.

### 3.1. Modeling by BRN

First, several different models were developed to determine the best setting for the control parameters of the BRN neural network, i.e. the layer size, spread, and number of neurons [50], [77]. It should be noted that the choice of values for these parameters greatly affects the network's convergence rate as well as accuracy. While some of these control parameters can be set based on the choices made in similar studies, many others have to be determined by trial and error [51]. Therefore, to determine the most suitable control parameters, a range was considered for each of the control data based on the opinions of experts and past disputes. Then by trial and error, the most suitable parameters were selected. Therefore, the models were built with 80, 100, 120, and 130 neurons, with the layer size set to 3 and spread set to 0.5, 1, and 2. Also the max iterations were considered the values of 100, 200, 450, and 750 in different models. The specifications of the 12 models developed in this stage are given in Table 3.

The simple ranking method of Zorlu *et al.* was then used to rank these models, reaching the ranking given in Table 4 [78].

**Table 3. Effect of control parameters of RBF network on performance of each model.**

| Model No. | Layer size | Spread | Number of neurons | Results of network for R <sup>2</sup> |      | Results of network for RMSE |      | Results of network for VAF |      |
|-----------|------------|--------|-------------------|---------------------------------------|------|-----------------------------|------|----------------------------|------|
|           |            |        |                   | Train                                 | Test | Train                       | Test | Train                      | Test |
| I         | 3          | 0.5    | 80                | 0.67                                  | 0.33 | 2.07                        | 2.88 | 49                         | 24   |
| II        | 3          | 0.5    | 100               | 0.63                                  | 0.4  | 2.09                        | 2.58 | 41                         | 23   |
| III       | 3          | 0.5    | 120               | 0.85                                  | 0.76 | 1.26                        | 1.95 | 84                         | 76   |
| IV        | 3          | 0.5    | 130               | 0.84                                  | 0.67 | 1.37                        | 2.08 | 82                         | 66   |
| V         | 3          | 1      | 80                | 0.68                                  | 0.5  | 2.17                        | 2.8  | 53                         | 40   |
| VI        | 3          | 1      | 100               | 0.83                                  | 0.72 | 1.32                        | 2.36 | 80                         | 72   |
| VII       | 3          | 1      | 120               | 0.99                                  | 0.91 | 0.29                        | 0.99 | 99                         | 90   |
| VIII      | 3          | 1      | 130               | 0.95                                  | 0.84 | 0.68                        | 1.54 | 95                         | 82   |
| IX        | 3          | 2      | 80                | 0.89                                  | 0.43 | 1.14                        | 2.6  | 88                         | 41   |
| X         | 3          | 2      | 100               | 0.94                                  | 0.84 | 0.77                        | 1.5  | 94                         | 84   |
| XI        | 3          | 2      | 120               | 0.94                                  | 0.82 | 0.77                        | 1.69 | 95                         | 82   |
| XII       | 3          | 2      | 130               | 0.88                                  | 0.71 | 1.19                        | 1.98 | 86                         | 70   |

As the results of Table 4 show, the best performance among these 12 models was observed in Model VII (score = 72): where the layer size was 3, the spread was 1, and the number of neurons was 120. It should be noted that the best number of iteration was 200. In contrast, the worst

performance was observed in Model I and Model II (score = 16). Figures 5-8 show the correlation between the observed data and data predicted by Model VII in the training and testing phases.

**Table 4. Ranking of each RBF network models.**

| Model No. | Layer size | Spread | Number of neurons | Results of network for R <sup>2</sup> |      | Results of network for RMSE |      | Results of network for VAF |      | Total rank |
|-----------|------------|--------|-------------------|---------------------------------------|------|-----------------------------|------|----------------------------|------|------------|
|           |            |        |                   | Train                                 | Test | Train                       | Test | Train                      | Test |            |
| I         | 3          | 0.5    | 80                | 3                                     | 2    | 4                           | 1    | 3                          | 3    | 16         |
| II        | 3          | 0.5    | 100               | 2                                     | 3    | 3                           | 4    | 2                          | 2    | 16         |
| III       | 3          | 0.5    | 120               | 7                                     | 9    | 7                           | 8    | 7                          | 9    | 47         |
| IV        | 3          | 0.5    | 130               | 6                                     | 6    | 5                           | 6    | 6                          | 6    | 35         |
| V         | 3          | 1      | 80                | 4                                     | 5    | 2                           | 2    | 4                          | 4    | 21         |
| VI        | 3          | 1      | 100               | 5                                     | 8    | 6                           | 5    | 5                          | 8    | 37         |
| VII       | 3          | 1      | 120               | 12                                    | 12   | 12                          | 12   | 12                         | 12   | 72         |
| VIII      | 3          | 1      | 130               | 11                                    | 11   | 11                          | 10   | 11                         | 10   | 64         |
| IX        | 3          | 2      | 80                | 9                                     | 4    | 9                           | 3    | 9                          | 5    | 39         |
| X         | 3          | 2      | 100               | 10                                    | 11   | 10                          | 11   | 10                         | 11   | 63         |
| XI        | 3          | 2      | 120               | 10                                    | 10   | 10                          | 9    | 11                         | 10   | 60         |
| XII       | 3          | 2      | 130               | 8                                     | 7    | 8                           | 7    | 8                          | 7    | 45         |

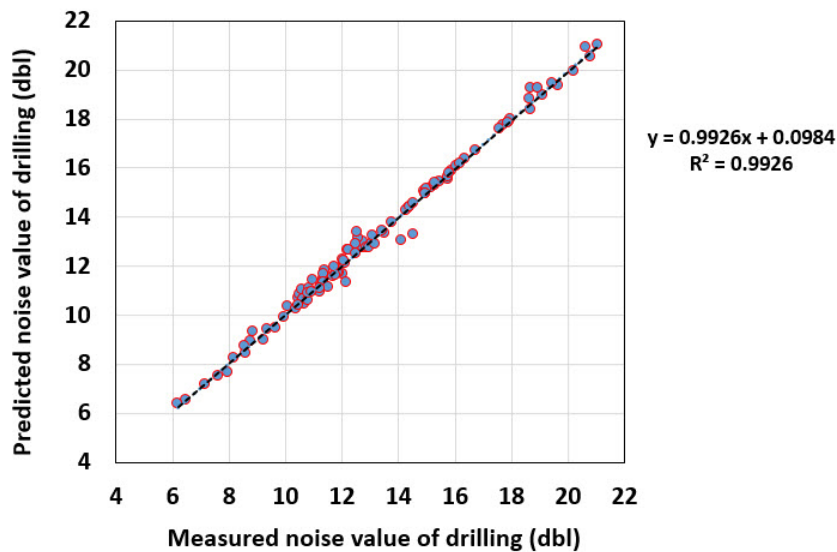


**Figure 5. Coefficient of determination between predicted values and actual measured values for training dataset of RBF model.**

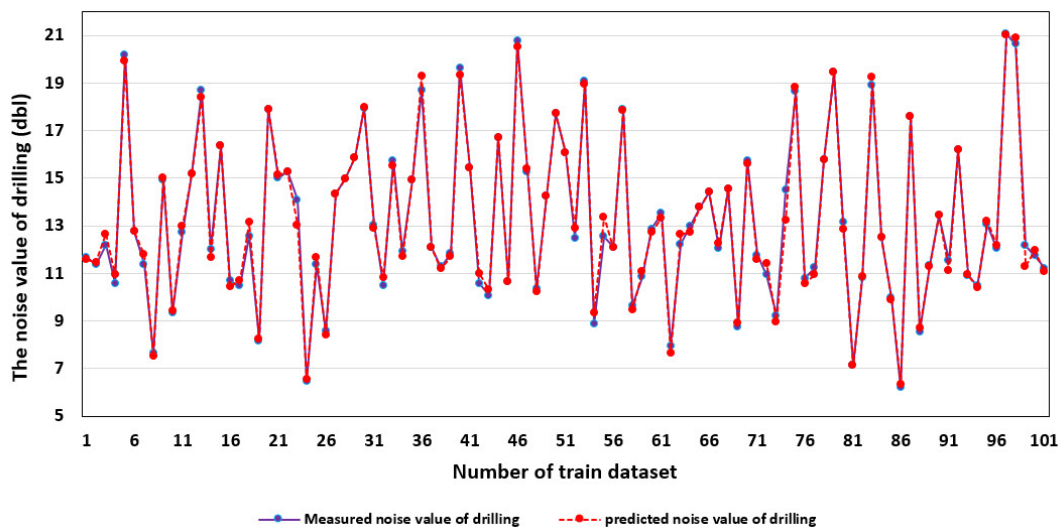


**Figure 6. Coefficient of determination between predicted values and actual measured values for testing dataset of RBF model.**

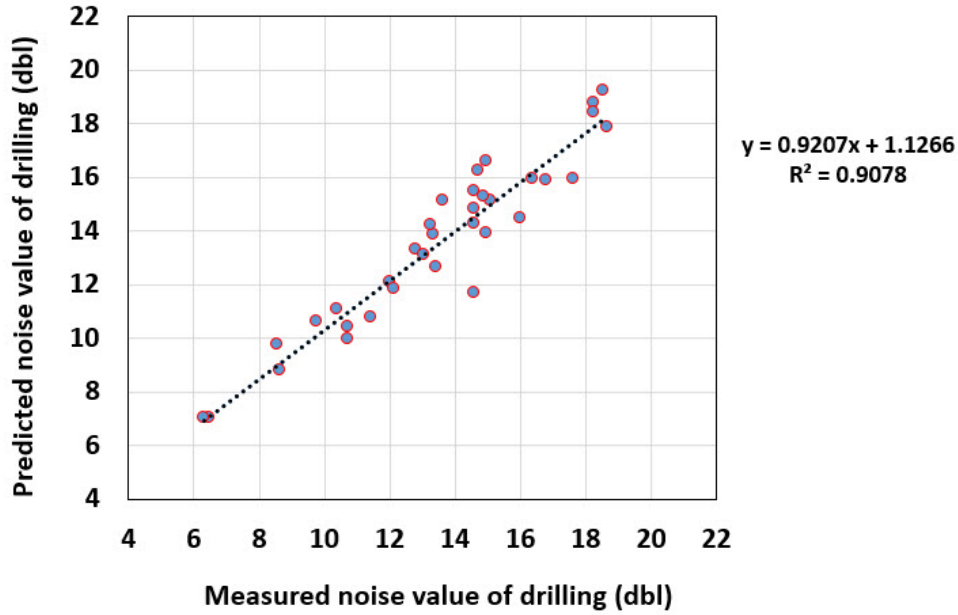


Figure 7. Comparison between measured and predicted noise value of drilling for testing dataset of RBF model.

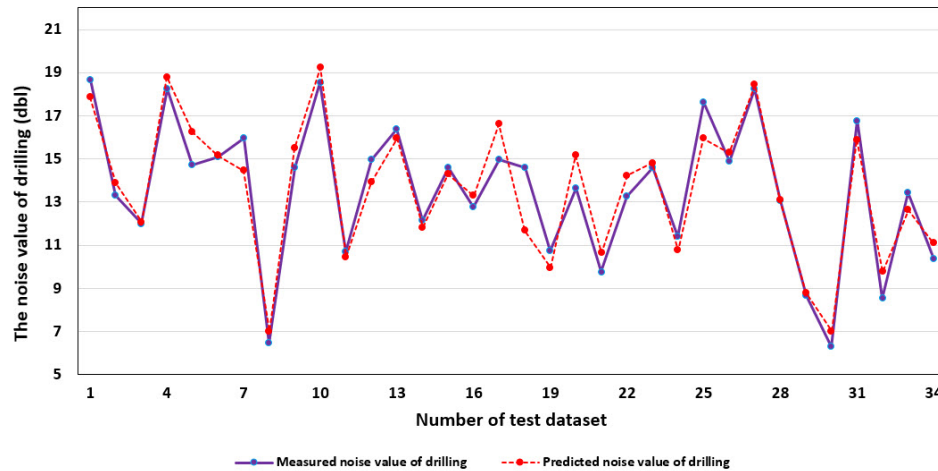


Figure 8. Comparison between measured and predicted noise value of drilling for testing dataset.

### 3.2. Modeling by ANFIS-FCM

At the first step in the ANFIS-FCM modeling procedure of this work, all datasets were normalized based on Equation 17.

$$X_{norm} = (X - X_{min}) / (X_{max} - X_{min}) \quad (17)$$

where  $X_{norm}$  is the normalized amount of the measured parameter.  $X$ ,  $X_{min}$ , and  $X_{max}$  are the measured values, the minimum and maximum amounts of the measured parameters, respectively [79]. It is worth mentioning that *genfis3* was applied for generating the fuzzy inference system (FIS) structure from a dataset based on the fuzzy c-means clustering technique in this modeling. The

FIS that was generated by *genfis3* is a Sugno-type FIS. Similar to modeling with RBF, a range of different values for ANFIS-SCM and ANFIS-FCM control parameters were considered with the consultation and opinion of experts. The optimal settings were then determined via iterative trial and error [72]. In fact, the control parameters play an important role in the rapid convergence of the algorithm with high accuracy. After constructing many models and evaluating the ability of the models to predict the amount of noise generated by performance indicators, the best developed model was determined. Some control parameters included the max epoch, initial step size, and number of clusters, which were considered a range for them

including the max epoch (10, 30, 50, and 100): initial step size (0.005, 0.01, and 0.02): and number of clusters (3, 5, 7, and 6). After trial and error and constructing several models, the best values for each of these parameters were selected as 30, 0.01, and 5 for the max epoch, initial step size, and number of clusters, respectively. Figure 9 shows the membership function of each input that was

considered by the ANFIS-FCM model. In addition, the coefficient of determination ( $R^2$ ) between the measured noise value of drilling and the predicted noise value of drilling for training and testing dataset is indicated in Figures 10 and 11, respectively. The results obtained show that the acceptable coefficients of determination were achieved by the ANFIS-FCM model.

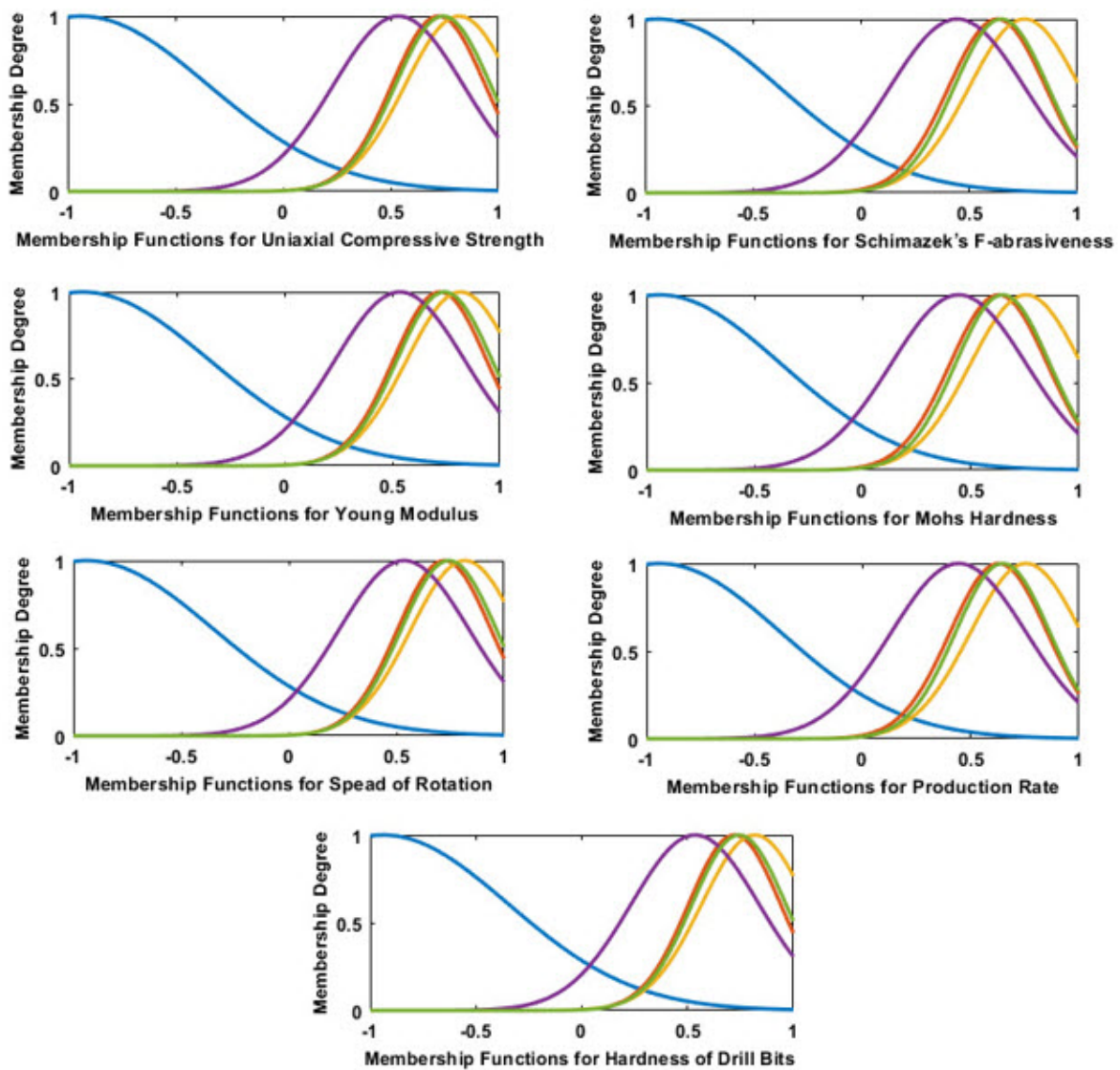


Figure 9. Membership function of inputs were generated by ANFIS-FCM model.

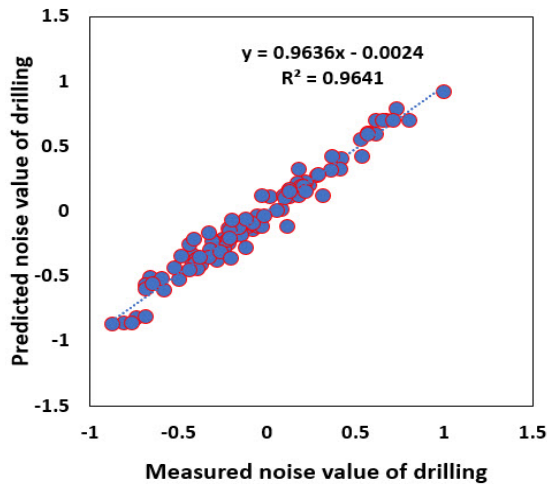


Figure 10. Comparison between measured and predicted noise value of drilling for training dataset of ANFIS-FCM model.

### 3.3. Modeling by ANFIS-SCM

As mentioned earlier, the first step in modeling with the ANFIS hybrid algorithm is to normalize the dataset. It should be noted that in this modeling, *genfis2* was used for generating the fuzzy inference system (FIS) structure from a dataset based on the subtractive clustering technique [72]. The FIS that was generated by *genfis2* is a Sugeno-type FIS. Then the most appropriate control parameters in the modeling were determined. Some control parameters were the max epoch, initial step size, and cluster center's range of influence (radii): which were considered a range for them including the max epoch (10, 20, 40, and 100); initial step size (0.01, 0.1, 0.2, 0.5, and 0.6); and cluster center's range of influence (0.6, 0.7, 0.8, and 0.9). After several models, the best developed ANFIS-

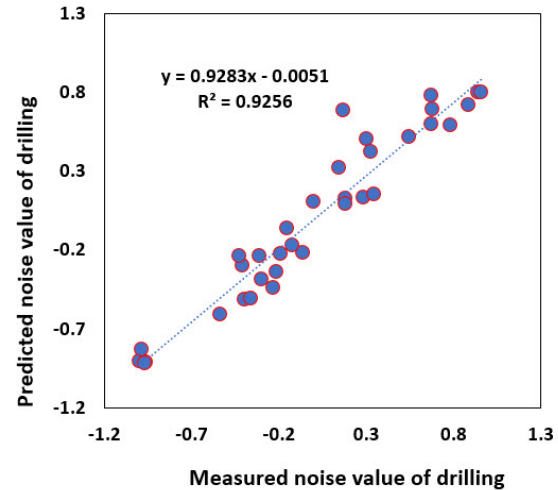


Figure 11. Comparison between measured and predicted noise value of drilling for testing dataset of ANFIS-FCM model.

SCM model was determined based on the values obtained from the performance indicators of the algorithm and a simple ranking method. The control parameters of the best developed ANFIS-SCM model included the max epoch = 40, initial step size = 0.5, and cluster center's range of influence (radii) equal to 0.8, which led to optimizing the convergence speed of the algorithm and accuracy in modeling. Figure 12 indicates that the membership function of each input that was generated by the ANFIS-FCM model. In addition, the coefficient of determination ( $R^2$ ) between the measured noise value of drilling and the predicted noise value of drilling for training and testing dataset is indicated in Figures 13 and 14, correspondingly. The results obtained demonstrate that the ANFIS-FCM model has acceptable coefficients of determination.

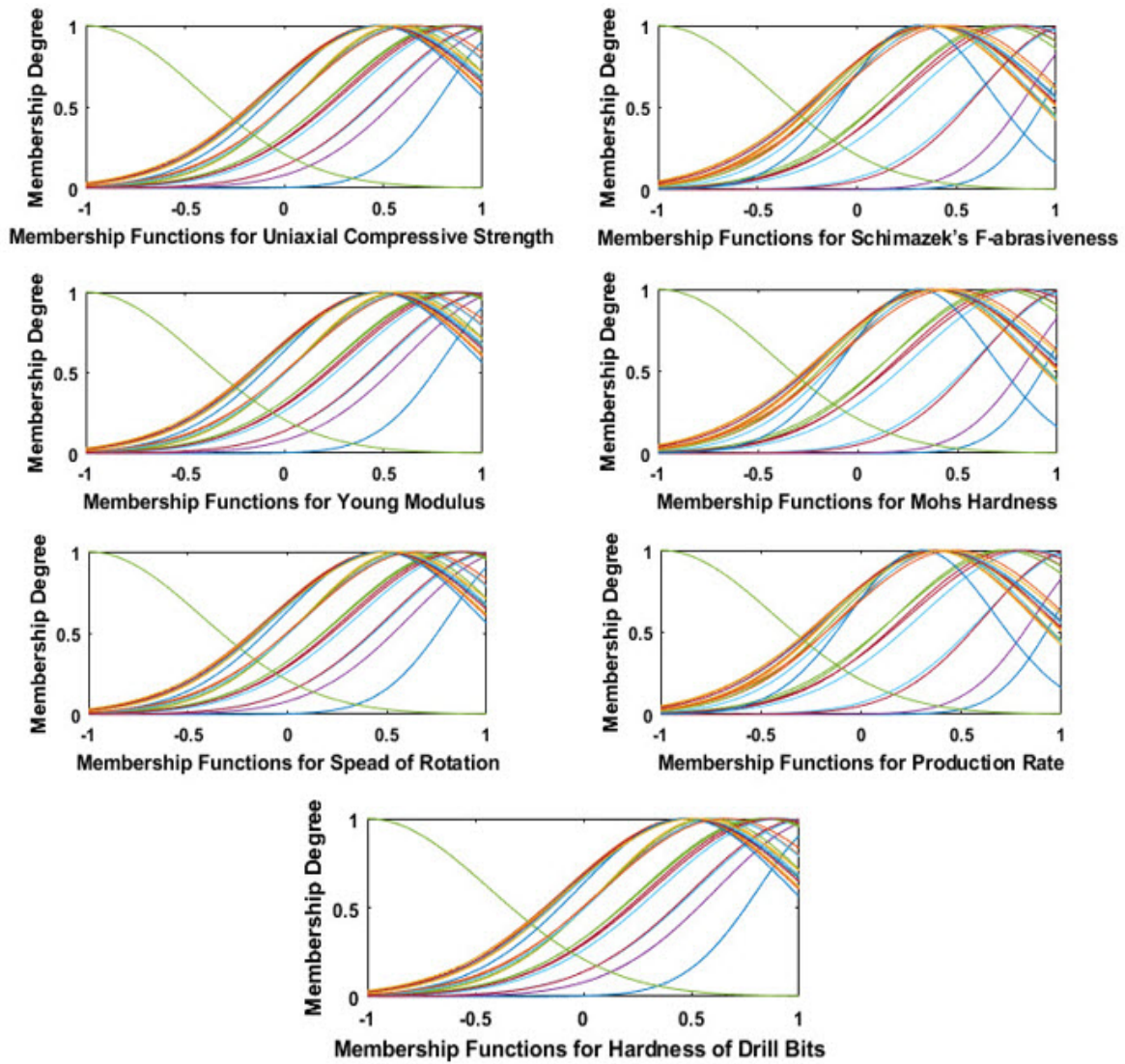


Figure 12. Membership function of inputs were generated by ANFIS-SCM model.

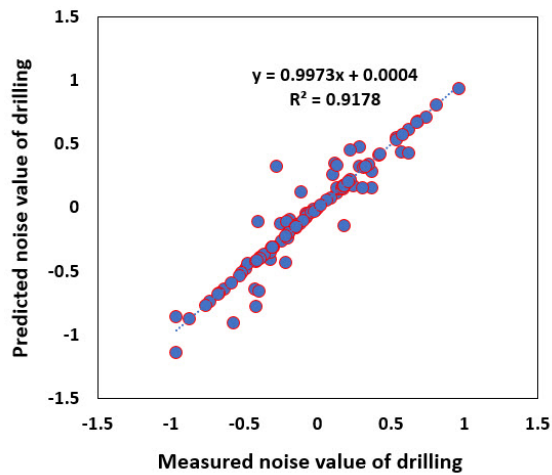


Figure 13. Comparison between measured and predicted noise value of drilling for training dataset of ANFIS-SCM model.

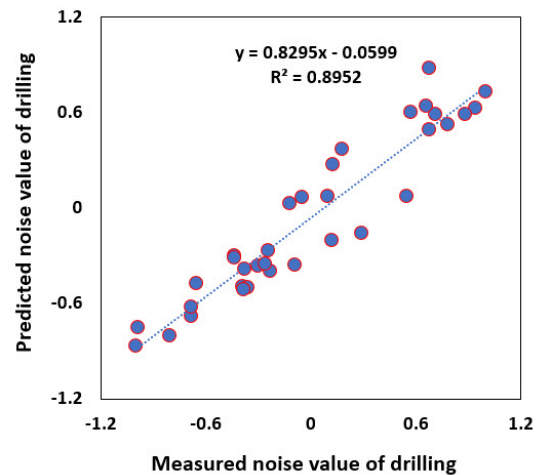


Figure 14. Comparison between measured and predicted noise value of drilling for testing dataset of ANFIS-SCM model.

#### 4. Discussion

As explained earlier, in this work, we conducted 135 laboratory tests on 5 types of rock and measured the noise level in each test. Then the modeling was done with 7 inputs: the rock's uniaxial compressive strength, Mohs hardness, Schimazek's F-abrasiveness factor, and Young modulus, the drill bit's hardness, and the drill machine's production rate and rotation speed. The

noise level was the only output. After developing multiple models with ANFIS-SCM, ANFIS-FCM, and RBF methods, the best model was obtained through each method, i.e. the one with the best mapping between input and output data and the highest correlation coefficient and lowest error was determined. Then the three best models were compared in terms of the performance measures described. The results of this comparison are presented in Table 5.

**Table 5. Comparison of results (R<sup>2</sup>, RMSE, VAF) of best developed models by three AI methods.**

| Best developed model | Results of network for R <sup>2</sup> |      | Results of network for RMSE |      | Results of network for VAF |      |
|----------------------|---------------------------------------|------|-----------------------------|------|----------------------------|------|
|                      | Train                                 | Test | Train                       | Test | Train                      | Test |
| RBF model            | 0.99                                  | 0.9  | 0.29                        | 0.99 | 99                         | 90   |
| ANFIS-FCM model      | 0.96                                  | 0.93 | 0.07                        | 0.15 | 96                         | 92   |
| ANFIS-SCM model      | 0.92                                  | 0.89 | 0.12                        | 0.17 | 91                         | 89   |

According to comparing the results of the three methods' performances, it is determined that although all methods have acceptable results in predicting the noise generated in rock drilling, ANFIS-FCM has a better performance compared to the other two models. In the studies that follow, the best-developed ANFIS-FCM model is used as a starting point to find out how the input parameters affect the amount of noise that is made.

In order to evaluate the effect of input parameters on the noise value of drilling, other different

scenarios were compared with the variation of input parameters and their results were compared with the results of the best developed ANFIS-FCM model. Table 6 shows the scenarios designed with different input parameters. After developing multiple models and their analysis, a comparison between the performance indices of the algorithm for four scenarios is shown in Table 7, as well as Figures 15 and 16, which show the correlation between the input and output data for each scenario in Table 6 for training and test data, respectively.

**Table 6. Four Scenarios with different inputs by best developed ANFIS-FCM model.**

| Scenario No. | Inputs                            |   |                              | Outputs                 |
|--------------|-----------------------------------|---|------------------------------|-------------------------|
|              | Mechanical properties of the rock | Operational characteristics of drilling machine | Characteristic of drill bits |                         |
| Scenario 1   | UCS, SF-a, YM, MH                 | PR, Speed of rotation                           | Hardness of drill bits       | Noise value of drilling |
| Scenario 2   | UCS, SF-a, YM, MH                 | PR, Speed of rotation                           | -                            | Noise value of drilling |
| Scenario 3   | UCS, SF-a, YM, MH                 | -   | Hardness of drill bits       | Noise value of drilling |
| Scenario 4   | -                                 | PR, Speed of rotation                           | Hardness of drill bits       | Noise value of drilling |

Scenario 1= Best developed ANFIS-FCM model with 7 inputs

**Table 7. Results of performance indices for all scenarios.**

| Scenario No. | Results of network for R <sup>2</sup> |      | Results of network for RMSE |       | Results of network for VAF |      |
|--------------|---------------------------------------|------|-----------------------------|-------|----------------------------|------|
|              | Train                                 | Test | Train                       | Test  | Train                      | Test |
| 1            | 0.96                                  | 0.93 | 0.077                       | 0.088 | 96                         | 92   |
| 2            | 0.6                                   | 0.57 | 0.282                       | 0.182 | 60                         | 56   |
| 3            | 0.91                                  | 0.88 | 0.127                       | 0.09  | 91                         | 88   |
| 4            | 0.64                                  | 0.6  | 0.265                       | 0.172 | 64                         | 60   |

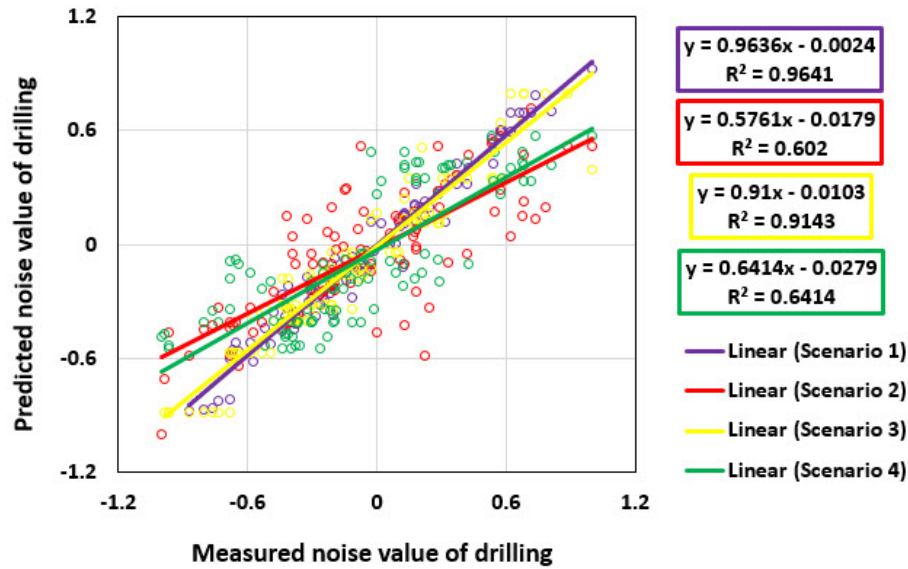


Figure 15. Coefficient of determination between predicted values and actual measured values for training dataset of 4 scenarios by ANFIS-FCM model.

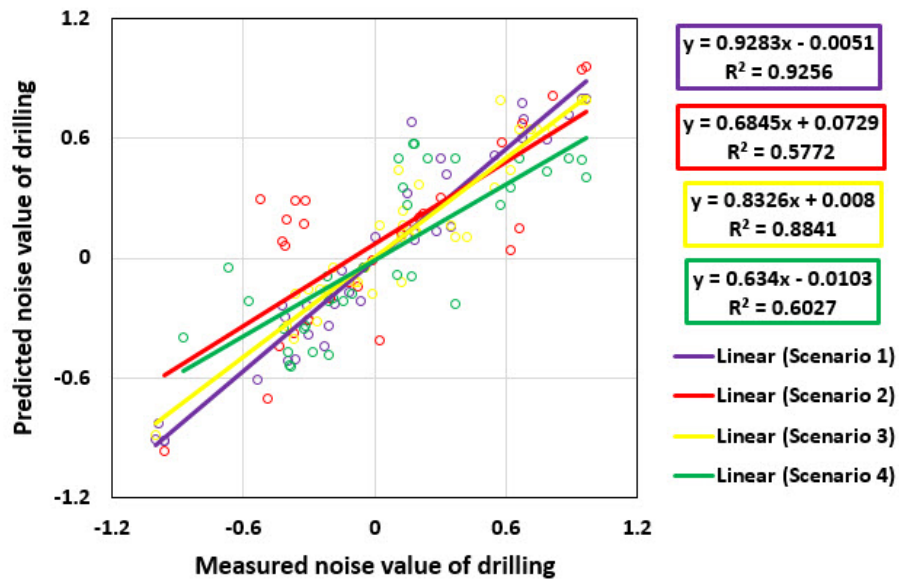


Figure 16. Coefficient of determination between predicted values and actual measured values for testing dataset of 4 scenarios by ANFIS-FCM model.

As shown in Table 7 and Figures 15 and 16, the best model developed by ANFIS-FCM exhibited a better mapping capability with higher correlation in scenario 1, where the effects of all the input parameters were considered. Also scenario 3 with 5 input parameters resulted in a better input-output mapping than scenario 1, which shows the importance of the hardness of the drill bit. Scenario 4 shows that the hardness of the drill bit, and the way the drilling machine works are not as important as the factors that were looked at in the first two scenarios. Also scenario 2 had the worst

mapping between the mechanical properties of the rock and the operational properties of the drilling machine as inputs and the noise of drilling as an output because the algorithm produced a lower correlation rate than in other cases. Due to the four scenarios, it can be concluded that drill bit hardness has the highest impact on noise level due to the mechanical properties of rock and operational parameters, and then mechanical properties have a greater impact on the amount of noise level due to the drilling. Therefore, it is recommended that the coating drill bits listed be used in rock drilling, and

it is suggested that the use of coating listed in rock-cutting machines can be used to reduce noise.

In addition, it should be noted that the correlation rate in scenario 1 was quite high. This shows that the algorithm is good at mapping inputs to outputs and supports the idea that all of these input parameters affect the drilling noise value at the same time.

At the end, it is important to stress that the proposed models with unique structures have properties sensitive to hard rocks, and cannot be easily applied to other kinds of rocks. Also when there is incomplete data, these algorithms are not able to provide modeling results with high strength and capability.

## 5. Conclusions

One of the major problems in the rock industry is the noise pollution generated by bit-rock interactions during drilling operations. In this work, the relationship between noise, rock properties, and drilling configuration was investigated by collecting and preparing five rock samples and subjecting them to a series of laboratory tests. During the laboratory tests, three main categories that affect the amount of generated noise in drilling operations including the four physical and mechanical properties of the rocks, two operational characteristics of the machine, and the hardness of the drill bits were measured. In addition, the noise levels were measured by the sound level meter in each test. In the next step, three artificial intelligence methods (ANFIS-FCM, ANFIS-SCM, and RBF) were used to look at the measurements from the lab and come up with different models for the relationship. In this modeling, the goal was to achieve the best mapping between output and input data. The comparison of the 12 models developed with different parameter configurations showed that Model VII with 120 neurons in 3 layers with a spread of 1 had the best score (72): and Model I and Model II had the worst scores (16) among these 12 models. In addition, the results of the models developed by the three methods were compared in terms of three performance measures. This comparison showed that the ANFIS-FCM model was more accurate than the models made by other methods.

Finally, the best model developed was reconstructed into multiple scenarios, each with a certain combination of input parameters, and the correlation between the inputs and the noise level generated during drilling was investigated. In this work, the best mapping was found in Scenario 1,

where all of the input parameters were used to build the model. This suggests that the drilling noise is affected by all the parameters measured in this work. The results also indicated that the type of rock and the drill bit had a bigger effect on drilling noise than the operating parameters of the drilling machine. This is something that is required to be taken into account when drilling operations are changed to reduce noise.

## Funding

This research work received no external funding.

## Conflicts of interest

The authors declare that they have no financial interests.

## References

- [1]. Careddu, N., Di Capua, G., and Siotto, G. (2019). Dimension stone industry should meet the fundamental values of geoethics. *Resources Policy*, 63, 101468.
- [2]. Mikaeil, R., Ozcelik, Y., Ataei, M., and Shaffiee Haghshenas, S. (2019). Application of harmony search algorithm to evaluate performance of diamond wire saw. *Journal of Mining and Environment*, 10 (1): 27-36.
- [3]. Shamsi, R., Amini, M.S., Dehghani, H., Bascompta, M., Jodeiri Shokri, B., and Entezam, S. (2022). Prediction of Fly-rock using Gene Expression Programming and Teaching-learning-based Optimization Algorithm. *Journal of Mining and Environment*, 13 (2): 391-406.
- [4]. Emami Meybodi, E., Hussain, S.K., Fatehi Marji, M., and Rasouli, V. (2022). Application of Machine Learning Models for Predicting Rock Fracture Toughness Mode-I and Mode-II. *Journal of Mining and Environment*, 13 (2): 465-480.
- [5]. Shaffiee Haghshenas, S., Mikaeil, R., Esmaeilzadeh, A., Careddu, N., and Ataei, M. (2022). Statistical Study to Evaluate Performance of Cutting Machine in Dimension Stone Cutting Process. *Journal of Mining and Environment*, 13 (1): 53-67.
- [6]. Alamdari, S., Basiri, M.H., Mousavi, A., and Soofastaei, A. (2022). Application of Machine Learning Techniques to Predict Haul Truck Fuel Consumption in Open-Pit Mines. *Journal of Mining and Environment*, 13(1): 69-85.
- [7]. Mikaeil, R., Esmaeilzadeh, A., Shaffiee Haghshenas, S., Ataei, M., Hajizadehigdir, S., Jafarpour, A., and Geem, Z. W. (2022). Evaluation of Dimension Stone According to Resistance to Freeze-Thaw Cycling to Use in Cold Regions. *Journal of Soft Computing in Civil Engineering*, 6 (1): 88-109.
- [8]. Mikaeil, R., Esmaeilzadeh, A., Aghaei, S., Haghshenas, S.S., Jafarpour, A., Mohammadi, J., and

- Ataei, M. (2021). Evaluating the sawability of rocks by chain-saw machines using the promethee technique. *Rudarsko-geološko-naftni zbornik (The Mining-Geological-Petroleum Engineering Bulletin)*: 36 (1).
- [9]. Khilman, T. (2004). Noise pollution in cities, Curitiba and Goteborg as examples. In proceeding of.
- [10]. Gradl, C., Eustes, A.W., and Thonhauser, G. (2008, September). An analysis of noise characteristics of drill bits. In *SPE Annual Technical Conference and Exhibition*. OnePetro.
- [11]. Karakurt, I., Aydın, G., and Aydın, K. Experimental and Statistical Investigation on Noise Level of Diamond Sawblades in Granitic Rock Sawing.
- [12]. Kumar, B.R., Vardhan, H., and Govindaraj, M. (2011). Sound level produced during rock drilling vis-à-vis rock properties. *Engineering geology*, 123 (4): 333-337.
- [13]. Obert, L. (1941). Use of sub-audible noises for prediction of rock bursts (Vol. 3555). US Department of the Interior, Bureau of Mines.
- [14]. Obert, Leonard, and Wilbur I. Duvall. Use of Sub-audible Noises for the Prediction of Rock Bursts: Part II. US Department of the Interior, Bureau of Mines, 1942.
- [15]. Knill, J.L., Franklin, J.A., and Malone, A.W. (1968, January). A study of acoustic emission from stressed rock. In *International Journal of Rock Mechanics and Mining Sciences & Geomechanics Abstracts (Vol. 5, No. 1, pp. 87-88)*. Pergamon.
- [16]. Hardy, H.R. (1972). Application of acoustic emission techniques to rock mechanics research. *Acoustic emission*.
- [17]. Marceau, J. and Moji, Y. (1973). Application of fracture mechanics testing to process control for adhesive bonding. Document D6-41145, Boeing Commercial Airplane Company.
- [18]. Byerlee, J., (1978). Friction of rocks In *Rock friction and earthquake prediction*. 615-626. Basel: Birkhäuser.
- [19]. Zborovjan, M. (2002). Identification of minerals from sound during drilling. Semestral Project. TU-Kosice.
- [20]. Zborovjan, M., Lesso, I., and Dorcak, L. (2003). Acoustic identification of rocks during drilling process. *Journal of Acta Montanistica Slovaca*, 8 (4): 91-93.
- [21]. Vardhan, H., Adhikari, G.R., and Raj, M.G. (2009). Estimating rock properties using sound levels produced during drilling. *International Journal of Rock Mechanics and Mining Sciences*, 46(3): 604-612.
- [22]. Yilmaz, I. and Kaynar, O. (2011). Multiple regression, ANN (RBF, MLP) and ANFIS models for prediction of swell potential of clayey soils. *Expert systems with applications*, 38 (5): 5958-5966.
- [23]. Kumar, B.R., Vardhan, H., and Govindaraj, M. (2011). Prediction of uniaxial compressive strength, tensile strength and porosity of sedimentary rocks using sound level produced during rotary drilling. *Rock mechanics and rock engineering*, 44 (5): 613-620.
- [24]. Kumar, B. R., Vardhan, H., Govindaraj, M., and Vijay, G.S. (2013). Regression analysis and ANN models to predict rock properties from sound levels produced during drilling. *International Journal of Rock Mechanics and Mining Sciences*, 58, 61-72.
- [25]. Kharaman, S., Delibalta, M.S., and Comakli, R. (2013). Noise level measurement test to predict the abrasion resistance of rock aggregates. *Fluctuation and Noise Letters*, 12(04): 1350021.
- [26]. Masood. (2015). Estimation of Sound Level Produced During Drilling of Igneous Rock Samples using a Portable Drill set-up. *Procedia earth and planetary science*, 11, 456-482.
- [27]. Delibalta, M.S., Kahraman, S.A.İ.R., and Comakli, R. (2015). The usability of noise level from rock cutting for the prediction of physico-mechanical properties of rocks. *Fluctuation and Noise Letters*, 14 (01): 1550006.
- [28]. Kivade, S. B., Murthy, C.S.N., and Vardhan, H. (2015). ANN models for prediction of sound and penetration rate in percussive drilling. *Journal of The Institution of Engineers (India): Series D*, 96 (2): 93-103.
- [29]. Kumar, C.V., Vardhan, H., Murthy, C.S., and Karmakar, N.C. (2019). Estimating rock properties using sound signal dominant frequencies during diamond core drilling operations. *Journal of Rock Mechanics and Geotechnical Engineering*, 11(4): 850-859.
- [30]. Yari, M. and Bagherpour, R. (2018). Investigating an innovative model for dimensional sedimentary rocks characterization using acoustic frequencies analysis during drilling. *Rudarsko-geološko-naftni zbornik*, 33(2): 17-25.
- [31]. Yari, M. and Bagherpour, R. (2018). Implementing acoustic frequency analysis for development the novel model of determining geomechanical features of igneous rocks using rotary drilling device. *Geotechnical and Geological Engineering*, 36 (3): 1805-1816.
- [32]. Yari, M., Bagherpour, R., and Khoshouei, M. (2019). Developing a novel model for predicting geomechanical features of carbonate rocks based on acoustic frequency processing during drilling. *Bulletin of Engineering Geology and the Environment*, 78 (3): 1747-1759.
- [33]. Piri, M., Mikaeil, R., Hashemolhosseini, H., Baghbanan, A., and Ataei, M. (2021). Study of the effect of drill bits hardness, drilling machine operating parameters and rock mechanical parameters on noise level in hard rock drilling process. *Measurement*, 167, 108447.

- [34]. Aryafar, A., Mikaeil, R., Doulati Ardejani, F., Shaffiee Haghshenas, S., and Jafarpour, A. (2019). Application of non-linear regression and soft computing techniques for modeling process of pollutant adsorption from industrial wastewaters. *Journal of Mining and Environment*, 10 (2): 327-337.
- [35]. Mohammadi, J., Ataei, M., Kakaie, R.K., Mikaeil, R., and Haghshenas, S.S. (2018). Prediction of the production rate of chain saw machine using the multilayer perceptron (MLP) neural network. *Civil Engineering Journal*, 4(7): 1575-1583.
- [36]. Behnood, A. and Golafshani, E.M. (2018). Predicting the compressive strength of silica fume concrete using hybrid artificial neural network with multi-objective grey wolves. *Journal of Cleaner Production*, 202, 54-64.
- [37]. Naderpour, H., Rafiean, A.H., and Fakharian, P. (2018). Compressive strength prediction of environmentally friendly concrete using artificial neural networks. *Journal of Building Engineering*, 16, 213-219.
- [38]. Dormishi, A., Ataei, M., Mikaeil, R., Khalokakaei, R., and Haghshenas, S.S. (2019). Evaluation of gang saws' performance in the carbonate rock cutting process using feasibility of intelligent approaches. *Engineering Science and Technology, an International Journal*, 22 (3): 990-1000.
- [39]. Hosseini, S.M., Ataei, M., Khalokakaei, R., Mikaeil, R., and Haghshenas, S.S. (2020). Study of the effect of the cooling and lubricant fluid on the cutting performance of dimension stone through artificial intelligence models. *Engineering Science and Technology, an International Journal*, 23 (1): 71-81.
- [40]. Fiorini Morosini, A., Shaffiee Haghshenas, S., Shaffiee Haghshenas, S., and Geem, Z.W. (2020). Development of a Binary Model for Evaluating Water Distribution Systems by a Pressure Driven Analysis (PDA) Approach. *Applied Sciences*, 10 (9): 3029.
- [41]. Amiri, M., Hasanipanah, M., and Amnieh, H.B. (2020). Predicting ground vibration induced by rock blasting using a novel hybrid of neural network and item set mining. *Neural Computing and Applications*, 1-19.
- [42]. Armaghani, D.J. and Asteris, P.G. (2021). A comparative study of ANN and ANFIS models for the prediction of cement-based mortar materials compressive strength. *Neural Computing and Applications*, 33 (9): 4501-4532.
- [43]. Lee, S. K., Lee, H., Back, J., An, K., Yoon, Y., Yum, K., and Hwang, S.U. (2021). Prediction of tire pattern noise in early design stage based on convolutional neural network. *Applied Acoustics*, 172, 107617.
- [44]. Dhiman, N.K., Singh, B., Saini, P.K., and Garg, N. (2021). Design of Optimal Noise Barrier for Metropolitan Cities using Artificial Neural Networks. In *Optimization Methods in Engineering* (pp. 359-375). Springer, Singapore.
- [45]. Akbarzadeh, M., Shaffiee Haghshenas, S., Jalali, S. M.E., Zare, S., and Mikaeil, R. (2022). Developing the Rule of Thumb for Evaluating Penetration Rate of TBM using Binary Classification. *Geotechnical and Geological Engineering*, 1-19.
- [46]. Er, M.J., Wu, S., Lu, J., and Toh, H.L. (2002). Face recognition with radial basis function (RBF) neural networks. *IEEE transactions on neural networks*, 13(3): 697-710.
- [47]. Mahanty, R.N. and Gupta, P.D. (2004). Application of RBF neural network to fault classification and location in transmission lines. *IEE Proceedings-Generation, Transmission and Distribution*, 151(2): 201-212.
- [48]. Seshagiri, S. and Khalil, H.K. (2000). Output feedback control of nonlinear systems using RBF neural networks. *IEEE Transactions on Neural Networks*, 11 (1): 69-79.
- [49]. Mohammadi, J., Ataei, M., Kakaie, R., Mikaeil, R., and Haghshenas, S.S. (2019). Performance evaluation of chain saw machines for dimensional stones using feasibility of neural network models. *Journal of Mining and Environment*, 10(4): 1105-1119.
- [50]. Hosseini, S.M., Ataei, M., Khalokakaei, R., Mikaeil, R., and Haghshenas, S.S. (2019). Investigating the Role of the Cooling and Lubricant Fluids on the Performance of Cutting Disks (Case Study: Hard Rocks). *Rudarsko-geološko-naftni zbornik*, 34 (2): 13-25.
- [51]. Mikaeil, R., Shaffiee Haghshenas, S., Ozcelik, Y., and Shaffiee Haghshenas, S. (2017). Development of intelligent systems to predict diamond wire saw performance. *Journal of Soft Computing in Civil Engineering*, 1 (2): 52-69.
- [52]. Aryafar, A., Mikaeil, R., Haghshenas, S.S., and Haghshenas, S.S. (2018). Application of metaheuristic algorithms to optimal clustering of sawing machine vibration. *Measurement*, 124, 20-31.
- [53]. Mikaeil, R., Haghshenas, S.S., and Hoseinie, S.H. (2018). Rock penetrability classification using artificial bee colony (ABC) algorithm and self-organizing map. *Geotechnical and Geological Engineering*, 36 (2): 1309-1318.
- [54]. Salemi, A., Mikaeil, R., and Haghshenas, S.S. (2018). Integration of finite difference method and genetic algorithm to seismic analysis of circular shallow tunnels (Case study: Tabriz urban railway tunnels). *KSCSE Journal of Civil Engineering*, 22 (5): 1978-1990.
- [55]. Mikaeil, R., Bakhshinezhad, H., Haghshenas, S.S., and Ataei, M. (2019). Stability analysis of tunnel support systems using numerical and intelligent simulations (case study: Kouhin Tunnel of Qazvin-

- Rasht Railway). Rudarsko-geološko-naftni zbornik, 34(2): 1-10.
- [56]. Haghshenas, S.S., Faradonbeh, R.S., Mikaeil, R., Haghshenas, S.S., Taheri, A., Saghatforoush, A., and Dormishi, A. (2019). A new conventional criterion for the performance evaluation of gang saw machines. *Measurement*, 146, 159-170.
- [57]. Mikaeil, R., Beigmohammadi, M., Bakhtavar, E., and Haghshenas, S.S. (2019). Assessment of risks of tunneling project in Iran using artificial bee colony algorithm. *SN Applied Sciences*, 1 (12): 1-9.
- [58]. Guido, G., Haghshenas, S.S., Haghshenas, S.S., Vitale, A., Gallelli, V., and Astarita, V. (2020). Development of a Binary Classification Model to Assess Safety in Transportation Systems using GMDH-Type Neural Network Algorithm. *Sustainability*, 12 (17): 6735.
- [59]. Guido, G., Haghshenas, S.S., Haghshenas, S.S., Vitale, A., Astarita, V., and Haghshenas, A.S. (2020). Feasibility of Stochastic Models for Evaluation of Potential Factors for Safety: A Case Study in Southern Italy. *Sustainability*, 12 (18): 7541.
- [60]. Noori, A.M., Mikaeil, R., Mokhtarian, M., Haghshenas, S.S., and Foroughi, M. (2020). Feasibility of intelligent models for prediction of utilization factor of TBM. *Geotechnical and Geological Engineering*, 38(3): 3125-3143.
- [61]. Naderpour, H. and Mirrashid, M. (2020). Moment capacity estimation of spirally reinforced concrete columns using ANFIS. *Complex & Intelligent Systems*, 6 (1): 97-107.
- [62]. Fiorini Morosini, A., Shaffiee Haghshenas, S., Shaffiee Haghshenas, S., Choi, D.Y., and Geem, Z.W. (2021). Sensitivity Analysis for Performance Evaluation of a Real Water Distribution System by a Pressure-driven Analysis Approach and Artificial Intelligence Method. *Water*, 13 (8): 1116.
- [63]. Golafshani, E.M. and Behnood, A. (2021). Predicting the mechanical properties of sustainable concrete containing waste foundry sand using multi-objective ANN approach. *Construction and Building Materials*, 291, 123314.
- [64]. Haghshenas, S.S., Haghshenas, S.S., Geem, Z.W., Kim, T.H., Mikaeil, R., Pugliese, L., and Troncone, A. (2021). Application of harmony search algorithm to slope stability analysis. *Land*, 10 (11): 1250.
- [65]. Singh, D., Upadhyay, R., Pannu, H. S., and Leray, D. (2021). Development of an adaptive neuro fuzzy inference system based vehicular traffic noise prediction model. *Journal of Ambient Intelligence and Humanized Computing*, 12 (2): 2685-2701.
- [66]. Senthilselvi, A., Duela, J. S., Prabavathi, R., and Sara, D. (2021). Performance evaluation of adaptive neuro fuzzy system (ANFIS) over fuzzy inference system (FIS) with optimization algorithm in de-noising of images from salt and pepper noise. *Journal of Ambient Intelligence and Humanized Computing*, 1-6.
- [67]. Naderpour, H. and Mirrashid, M. (2020). Moment capacity estimation of spirally reinforced concrete columns using ANFIS. *Complex & Intelligent Systems*, 6 (1): 97-107.
- [68]. Armaghani, D.J., Harandizadeh, H., and Momeni, E. (2021). Load carrying capacity assessment of thin-walled foundations: an ANFIS-PNN model optimized by genetic algorithm. *Engineering with Computers*, 1-23.
- [69]. Jang, J. S. (1993). ANFIS: adaptive-network-based fuzzy inference system. *IEEE transactions on systems, man, and cybernetics*, 23 (3): 665-685.
- [70]. Jang, J.S.R., Sun, C.T., and Mizutani, E. (1997). Neuro-fuzzy and soft computing-a computational approach to learning and machine intelligence [Book Review]. *IEEE Transactions on automatic control*, 42(10): 1482-1484.
- [71]. Dormishi, A.R., Ataei, M., Khaloo Kakaie, R., Mikaeil, R., and Shaffiee Haghshenas, S. (2019). Performance evaluation of gang saw using hybrid ANFIS-DE and hybrid ANFIS-PSO algorithms. *Journal of Mining and Environment*, 10(2): 543-557.
- [72]. Mikaeil, R., Haghshenas, S.S., Ozcelik, Y., and Gharegheshlagh, H.H. (2018). Performance evaluation of adaptive neuro-fuzzy inference system and group method of data handling-type neural network for estimating wear rate of diamond wire saw. *Geotechnical and Geological Engineering*, 36 (6): 3779-3791.
- [73]. Mikaeil, R., Haghshenas, S.S., Haghshenas, S.S., and Ataei, M. (2018). Performance prediction of circular saw machine using imperialist competitive algorithm and fuzzy clustering technique. *Neural Computing and Applications*, 29 (6): 283-292.
- [74]. Faradonbeh, R.S., Haghshenas, S.S., Taheri, A., and Mikaeil, R. (2020). Application of self-organizing map and fuzzy c-mean techniques for rock-burst clustering in deep underground projects. *Neural Computing and Applications*, 32 (12): 8545-8559.
- [75]. Mikaeil, R., Haghshenas, S.S., and Sedaghati, Z. (2019). Geotechnical risk evaluation of tunneling projects using optimization techniques (case study: The second part of Emamzade Hashem tunnel). *Natural Hazards*, 97 (3): 1099-1113.
- [76]. Fattahi, H. (2017). Prediction of slope stability using adaptive neuro-fuzzy inference system based on clustering methods. *Journal of Mining and Environment*, 8 (2): 163-177.
- [77]. Asgari, M., Kheyroddin, A., and Naderpour, H. (2017). A proposal model for estimation of project success in terms of radial based neural networks: a case study in Iran. *Civil Engineering Journal*, 3(10): 904-919.

[78]. Zorlu, K., Gokceoglu, C., Ocakoglu, F., Nefeslioglu, H.A., and Acikalin, S.J.E.G. (2008). Prediction of uniaxial compressive strength of sandstones using petrography-based models. *Engineering Geology*, 96 (3-4): 141-158.

[79]. Fattahi, H. (2016). Adaptive neuro fuzzy inference system based on fuzzy c-means clustering algorithm, a technique for estimation of TBM penetration rate. *Iran University of Science & Technology*, 6 (2): 159-171.

## یک روش تجربی-هوشمند برای پیش بینی مقدار نوبز مته کاری در صنعت سنگ های ساختمانی

رضا میکائیل<sup>۱</sup>، مصطفی پیری<sup>۲</sup>، سینا شفیعی حق شناس<sup>۳\*</sup>، نیکولا کاردو<sup>۴</sup> و حمید هاشم الحسینی<sup>۵</sup>

۱- دانشکده محیط زیست، گروه مهندسی معدن، دانشگاه صنعتی ارومیه، ارومیه، ایران

۲- گروه مهندسی معدن، دانشگاه صنعتی اصفهان (IUT)، اصفهان، ایران

۳- گروه مهندسی عمران، دانشگاه کالابریا، ۸۷۰۳۶، رنده، ایتالیا

۴- گروه عمران، مهندسی محیط زیست و معماری (DICAAR)، دانشگاه کالیاری؛ موسسه زمین شناسی محیطی و مهندسی زمین، Via Marengo 2, CNR-IGAG، ۰۹۱۲۳ کالیاری، ایتالیا

۵- گروه مهندسی عمران، دانشگاه صنعتی اصفهان (IUT)، اصفهان، ایران

ارسال ۲۰۲۲/۰۷/۱۰، پذیرش ۲۰۲۲/۰۹/۱۲

\* نویسنده مسئول مکاتبات: Sina.shaffieha.ghshenas@unical.it

### چکیده:

سر و صدای حفاری در تجارت سنگ ساختمانی هم برای محل کار و هم برای افرادی که در آنجا کار می کنند غیرقابل تحمل است. به منظور کاهش اثرات منفی مته کاری بر سلامت محیط زیست، نوبز مته کاری باید اندازه گیری، ارزیابی و کنترل شود. هدف اصلی این کار بررسی یک روش تجربی-هوشمند برای پیش بینی مقدار نوبز مته کاری در صنعت سنگ های ساختمانی است. برای این منظور ۱۳۵ آزمایش آزمایشگاهی بر روی پنج نوع سنگ (چهار نوع سنگ سخت و یک نوع سنگ نرم) طراحی شده و نتایج آن در مرحله اول اندازه گیری می شوند. در مرحله دوم، با توجه به مسائل پیش بینی نشده و نامشخص در این مورد، رویکردهای هوش مصنوعی (AI) اعمال شده و مدل سازی با استفاده از سه سیستم هوشمند (IS) یعنی یک سیستم استنتاج عصبی فازی تطبیقی (ANFIS-FCM) و FCM و یک سیستم استنتاج عصبی فازی تطبیقی-FCM (ANFIS-FCM) و شبکه عصبی مبتنی بر عملکرد شبکه (RBF). ۷۵ درصد نمونه ها برای آموزش و بقیه برای تست در نظر گرفته شده اند. چندین مدل ساخته شده است و نتایج نشان می دهد که اگرچه تفاوت معنی داری بین مدل ها بر اساس شاخص های عملکرد وجود ندارد، مدل پیشنهادی ANFIS-SCM می تواند به عنوان ابزاری کارآمد در ارزیابی نوبز مته کاری در نظر گرفته شود. در نهایت، چندین سناریو با حالت های ورودی مختلف طراحی شده است و نتایج به دست آمده ثابت می کند که انواع سنگ و مته ها از ویژگی های عملیاتی دستگاه مهم تر هستند.

**کلمات کلیدی:** نوبز مته کاری، سنگ ساختمانی، سنگ سخت، سیستم های هوشمند، ANFIS-SCM، ANFIS-FCM، RBF.